

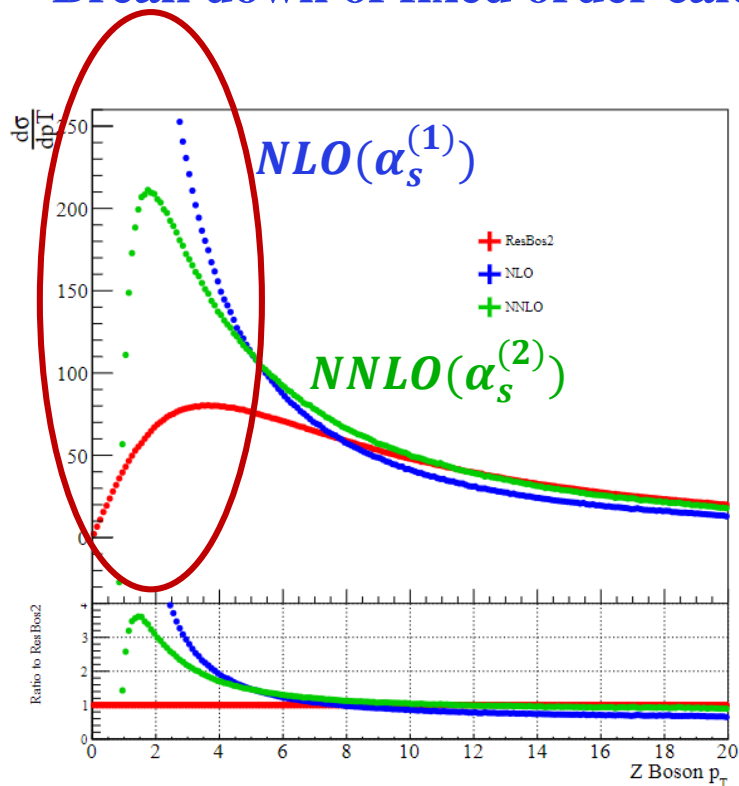


Nonperturbative fit in resummation calculation

Joshua Isaacson, Yao Fu, C.-P. Yuan

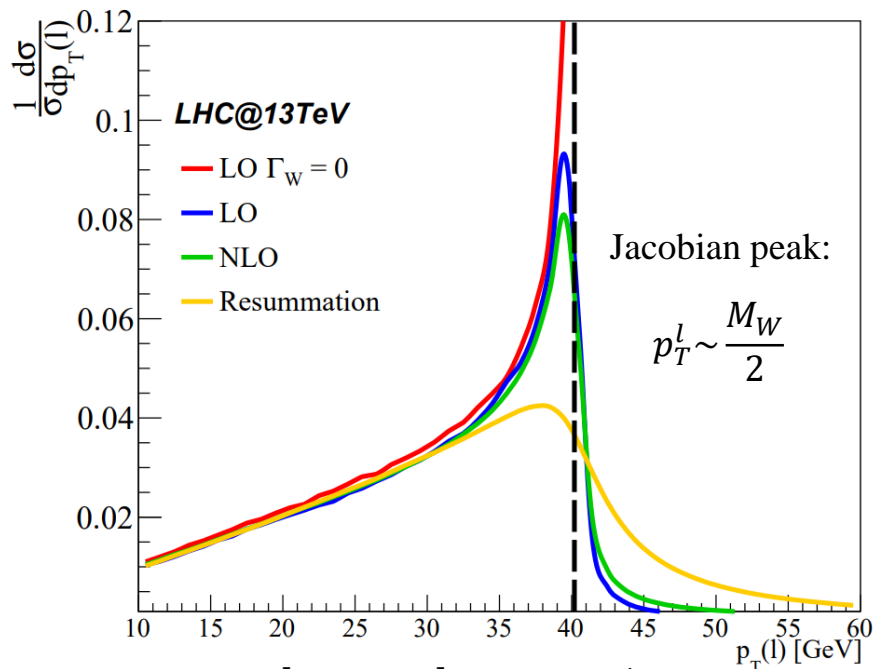
Resummation calculation in p_T modeling

➤ Break down of fixed order calculation



$$\frac{d\sigma}{dq_T^2} \sim \frac{1}{q_T^2} \sum_{n=1}^{\infty} \sum_{m=0}^{2n-1} \alpha_s^n \ln^m \frac{Q^2}{q_T^2}$$

Fixed order calculation breaks down when $q_T \rightarrow 0$, after q_T resummation, the q_T distribution can agree with data.



$$\frac{d\sigma}{dp_T^l} \sim \frac{d\sigma}{d\cos\theta} \frac{1}{\sqrt{1 - \frac{4p_T^l{}^2}{\hat{s}}}}$$

Lepton kinematics are also sensitive to the p_T modeling.

Resummation calculation in EW parameter measurement

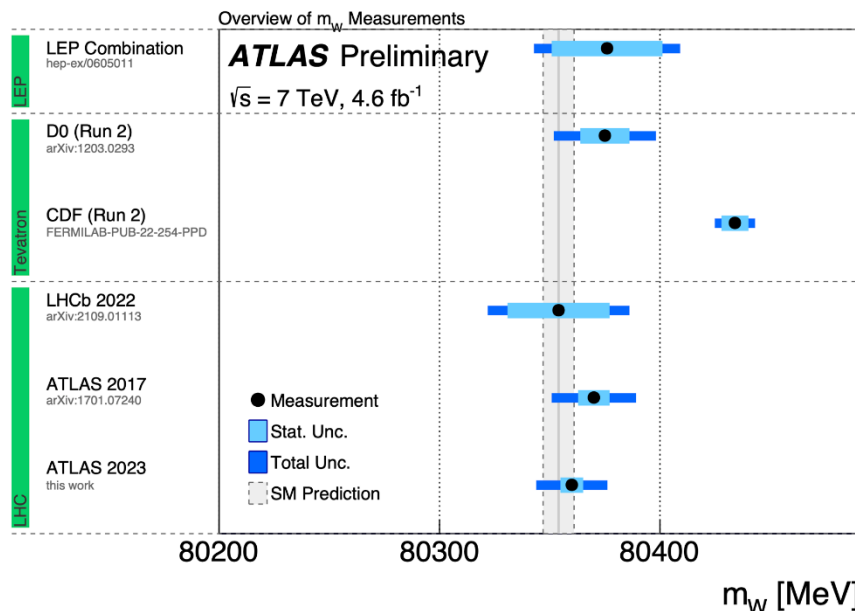
➤ ResBos (Resummation for Bosons)

Event generator.

Precision Electroweak Physics at Hadron Colliders

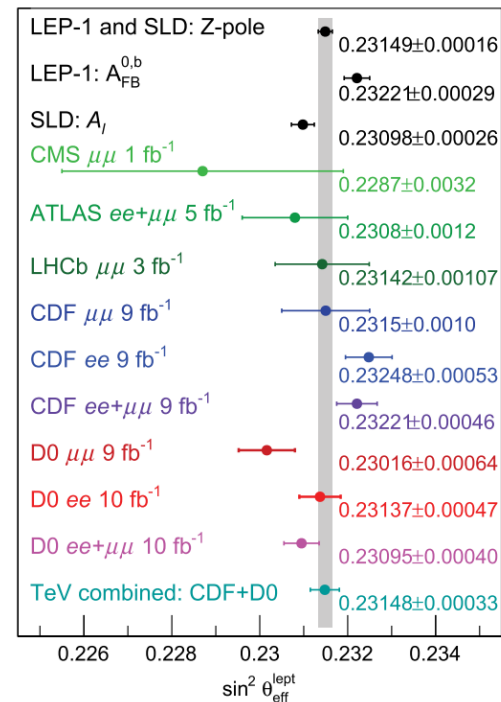
➤ Measurement of electroweak parameter is sensitive to p_T modeling

W mass measurement



<https://cds.cern.ch/record/2853290/files/ATLAS-CONF-2023-004.pdf>

$\sin^2 \theta_{eff}^l$ measurement



[PhysRevD.97.112007](https://arxiv.org/abs/1907.07801)

Measurement of W boson mass and $\sin^2 \theta_{eff}^l$ at hadron collider both need resummation calculation.

CSS q_T -resummation formalism and ResBos program

➤ CSS resummation formalism

$$\frac{d\sigma}{dQ^2 dq_T^2 dy} = \frac{H}{(2\pi)^2} \int d^2b e^{i\vec{q}_T \cdot \vec{b}} e^{-S(Q,b)} \times \sum_j C_j \left(\frac{C_1}{C_2 b}, Q, x_1 \right) C_j \left(\frac{C_1}{C_2 b}, Q, x_2 \right) + Y(q_T, Q, x_1, x_2),$$

$$S(Q, b) = \int_{C_1^2/b^2}^{C_2^2 Q^2} \frac{d\mu^2}{\mu^2} \left(A(g_s(\mu), C_1) \log \frac{C_2^2 Q^2}{\mu^2} + B(\mu), C_1, C_2 \right).$$

$$A \equiv \sum_{n=1}^{\infty} \left(\frac{\alpha_s}{\pi} \right)^n A^{(n)}$$

$$B \equiv \sum_{n=1}^{\infty} \left(\frac{\alpha_s}{\pi} \right)^n B^{(n)}$$

$$C \equiv \sum_{n=1}^{\infty} \left(\frac{\alpha_s}{\pi} \right)^n C^{(n)}$$

$A^{(n)}$, $B^{(n)}$, and $C^{(n)}$ are calculated order by order.

	Order	Boundary Condition (C)	Anomalous Dimension		Fixed Order Matching (Y)
			γ_i (B)	Γ_{cusp} (A)	
	LL	1	-	1-loop	-
	NLL	1	1-loop	2-loop	-
ResBos	NLL' (+ NLO)	α_s	1-loop	2-loop	α_s
➔	NNLL (+ NLO)	α_s	2-loop	3-loop	α_s
	NNLL' (+ NNLO)	α_s^2	2-loop	3-loop	α_s^2
ResBos2	N ³ LL (+ NNLO)	α_s^2	3-loop	4-loop	α_s^2
➔	N ³ LL' (+ N ³ LO)	α_s^3	3-loop	4-loop	α_s^3
	N ⁴ LL (+ N ³ LO)	α_s^3	4-loop	5-loop	α_s^3

Nonperturbative part in CSS formalism

➤ Nonperturbative function

When $b \rightarrow \infty$, $q_T \rightarrow 0$, the calculation is nonperturbative.

$$b^* = \frac{b}{\sqrt{1 + \frac{b^2}{b_{max}^2}}}, \quad \mathcal{S}(Q, b) = \int_{C_1^2/b^2}^{C_2^2 Q^2} \frac{d\mu^2}{\mu^2} \left(A(g_s(\mu), C_1) \log \frac{C_2^2 Q^2}{\mu^2} + B(\mu), C_1, C_2 \right).$$

Final resummation formalism is

$$\frac{d\sigma}{dQ^2 dq_T^2 dy} = \sum_{i,j} \frac{H}{(2\pi)^2} \int d^2b e^{iq_T \cdot \vec{b}} e^{-S_{\text{pert}}} e^{-S_{NP}} C \otimes f_i C \otimes f_j,$$

Q -dependence \sqrt{s} -dependence

BLNY: $e^{-S_{NP}} = \exp \left[-g_1 - g_2 \ln\left(\frac{Q}{2Q_0}\right) - g_1 g_3 \ln(100x_1 x_2) \right] b^2,$ [hep-ph/0212159](https://arxiv.org/abs/hep-ph/0212159)

SIYY: $e^{-S_{NP}} = \exp \left[-g_1 b^2 - g_2 \ln(b/b_*) \ln(Q/Q_0) - g_3 b^2 \left((x_0/x_1)^\lambda + (x_0/x_2)^\lambda \right) \right],$ [arxiv: 1406.3073](https://arxiv.org/abs/1406.3073)

Nonperturbative function depends on collision energy \sqrt{s} and energy scale Q .

New nonperturbative function is needed

- The calculation order of ResBos is improved from $A=3, B=2, C=1$ (NNLL) to $A=4, B=3, C=2$ (N3LL), the nonperturbative function is needed to be updated.
- Previous nonperturbative function fitting only include low energy data and Tevatron data. Currently ATLAS, CMS, and LHCb collaboration have published more precise p_T data. Including the impact from new data is important.
- p_T data from ATLAS and CMS has rapidity dependence, and the data from LHCb is obtained in high rapidity region. It's good to test whether the nonperturbative function has rapidity dependence.

Rapidity-dependent nonperturbative formalism

➤ IFY functional form

$$S_{IFY} = g_1 + (g_2 + g_3 b^2) \log \left(\frac{Q}{M_Z} \right) + g_4 \log \left(\frac{1960}{\sqrt{s}} \right) + g_5 (\tanh (g_6 y_{\text{Max}}) + \tanh (g_6 (|y| - y_{\text{Max}}))),$$

- y_{max} is the maximum allowed rapidity for a given experimental setup, it's fixed to 5 here.
- The term proportional to g_4 is chosen such that at the Tevatron, the dominate contribution comes to the non-perturbative function comes from g_1 .
- The term proportional to g_5 is chosen such that for $y = 0$ the contribution from this term vanishes.
- The g_3 is fixed to 0 in the fit.

Data list in nonperturbative fit

Experiment	\sqrt{s}	Cuts	N_{pts}
CDF Run 1 [64]	1800 GeV	$66 \text{ GeV} < M_{\ell\ell} < 116 \text{ GeV}$	32
CDF Run 2 [65]	1960 GeV	$66 \text{ GeV} < M_{\ell\ell} < 116 \text{ GeV}$	41
D0 Run 1 [66]	1800 GeV	$66 \text{ GeV} < M_{\ell\ell} < 116 \text{ GeV}$	15
D0 Run 2 [67]	1960 GeV	$66 \text{ GeV} < M_{\ell\ell} < 116 \text{ GeV}$	8
E288 200 [68]	19.4 GeV	$4 \text{ GeV} < M_{\ell\ell} < 8 \text{ GeV}, y = 0.4$	28
E288 300 [68]	23.8 GeV	$4 \text{ GeV} < M_{\ell\ell} < 8 \text{ GeV}, 11 \text{ GeV} < M_{\ell\ell} < 12 \text{ GeV}, y = 0.21$	35
E288 400 [68]	27.4 GeV	$5 \text{ GeV} < M_{\ell\ell} < 8 \text{ GeV}, 11 \text{ GeV} < M_{\ell\ell} < 14 \text{ GeV}, y = 0.03$	42
E605 [69]	38.8 GeV	$7 \text{ GeV} < M_{\ell\ell} < 9 \text{ GeV}, 10.5 \text{ GeV} < M_{\ell\ell} < 14 \text{ GeV}, E_z = 0.1 \text{ GeV}$	35
R209 [70]	62 GeV	$5 \text{ GeV} < M_{\ell\ell} < 11 \text{ GeV}, 0.1 < x < 0.8$	10
ATLAS [71]	8000 GeV	$66 \text{ GeV} < M_{\ell\ell} < 116 \text{ GeV}, p_{T_\ell} > 20 \text{ GeV}, \eta_\ell < 2.4$	48
CMS [2]	13000 GeV	$76.1876 \text{ GeV} < M_{\ell\ell} < 106.1876 \text{ GeV}, p_{T_\ell} > 25 \text{ GeV}, \eta_\ell < 2.4$	80
LHCb [72]	13000 GeV	$60 \text{ GeV} < M_{\ell\ell} < 120 \text{ GeV}, p_{T_\ell} > 20 \text{ GeV}, 2.0 < \eta_\ell < 4.5$	10

New data

TABLE II. A list of all experiments used for the non-perturbative fit. The first column gives the name of the experiment, the second gives the center of mass energy, the third describes the experimental cuts applied for each set of events, and the last column gives the total number of datapoints for each experiment.

Only $p_T < 20 \text{ GeV}$ data will be used in the fit, since the resummation calculation is mainly focus on low p_T region.

Fitting strategy

➤ χ^2 function

$$\chi_E^2 = \sum_{k=1}^{N_{pt}} \frac{1}{s_k^2} \left(D_k - T_k(g) - \sum_{\alpha=1}^{N_\lambda} \lambda_\alpha \beta_{k\alpha} \right)^2 + \sum_{\alpha=1}^{N_\lambda} \lambda_\alpha^2.$$

D_k : Central value of data.

$T_k(g)$: Theoretical prediction of the data.

s_k^2 : Quadratic sum of the statistical uncertainty and uncorrelated uncertainty.

$\beta_{k\alpha}$: The matrix for correlated uncertainty.

λ_α : Nuisance parameters.

–0.5 χ^2 is used to be as the logarithm of Gaussian function in the likelihood fitting. The Bayesian Analysis Toolkit (BAT) package is used to perform the fitting.

➤ PDF uncertainty

The PDF uncertainty of each data point is treated as uncorrelated, which is also included in the χ^2 function.

The PDF uncertainties of ATLAS, CMS, and LHCb data set are divided by a factor of 3, to increase the weight of the rapidity dependence data in the global fitting. After fitting, the χ^2 are calculated again using the normal PDF uncertainty for each data set.

Scale choice

➤ Resummation scale and fixed order scale

Resummation scale: $C_1(b_0), C_2(1), C_3(4b_0)$ $b_{max} = b_0$ $b_0 = 2e^{-\gamma_E}$

Fixed order scale: $\mu_R(M_T), \mu_F(M_T)$ $M_T = \sqrt{p_T^2 + Q^2}$

The choice of $C_3 = 4b_0$ is to ensure that the ratio C_3/b^* is always greater than the cutoff scale for the PDF to ensure that there is no extrapolation needed in the calculation.

$$b_0 \approx 1.123$$

$$b_{max} = b_0 \approx 1.123$$

$$Q_0(CT18NNLO) = 1.3$$

$$(C_3/b^*)_{min} = C_3/b_{max} = 4 > 1.3$$

$$b^* = \frac{b}{\sqrt{1 + \frac{b^2}{b_{max}^2}}}$$

$C_2(1)$	$\mu_R(M_T)$	$\mu_F(M_T), C_1(b_0), C_3(4b_0)$
1	1	1
0.5	1	1
1	0.5	1
1	1	0.5
0.5	0.5	1
0.5	1	0.5
1	0.5	0.5
0.5	0.5	0.5
2	1	1
1	2	1
1	1	2
2	2	1
2	1	2
1	2	2
2	2	2



Scale variation in the estimation of scale uncertainty

In original BLNY, $b_{max} = 0.5$

g_5 determination in the nonperturbative fit

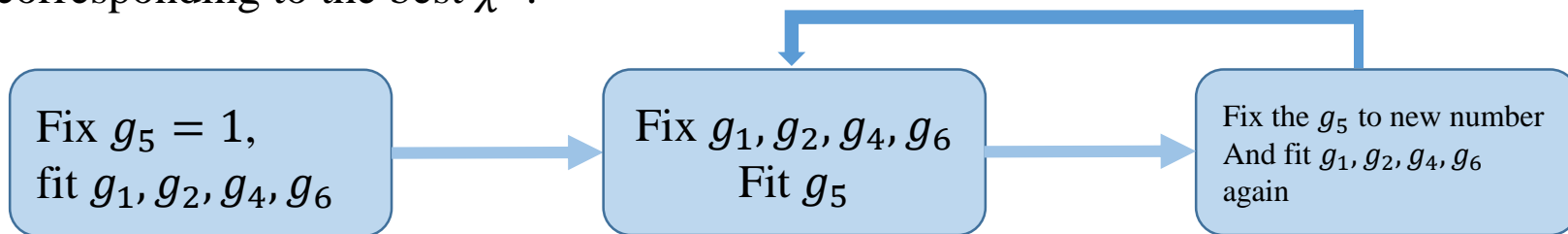
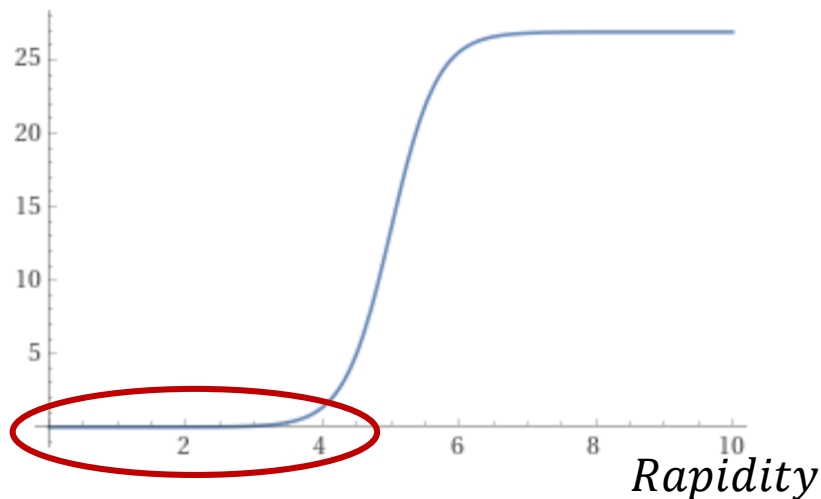
The g_1 and g_5 are highly correlated in the fit, because most of the data doesn't have rapidity dependence or in low rapidity region. The g_5 term in low rapidity region is almost flat and play the same role as the g_1

$$g_5(\tanh(g_6 y_{Max}) + \tanh(g_6(|y| - y_{Max})))$$

We fix the $g_5 = 1$ at first, and only fix for g_1, g_2, g_4, g_6 parameters.

Then fix g_1, g_2, g_4, g_6 parameters, fit for g_5 .

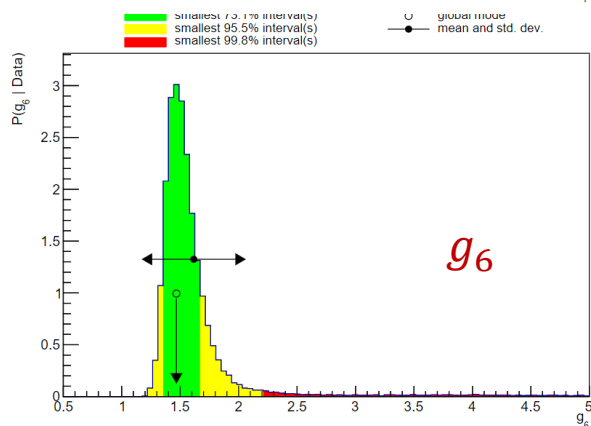
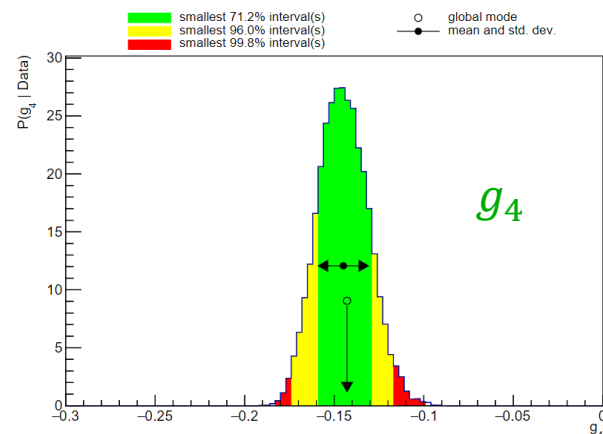
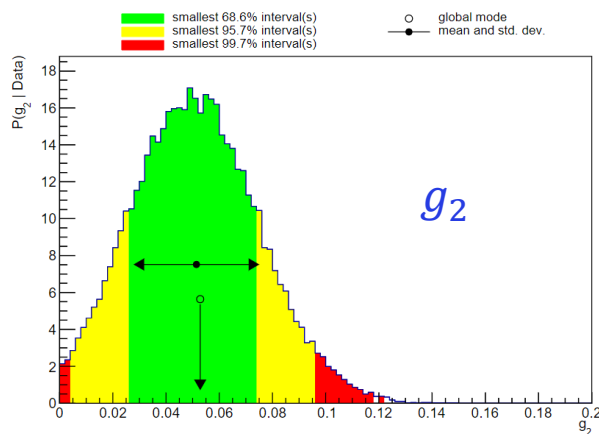
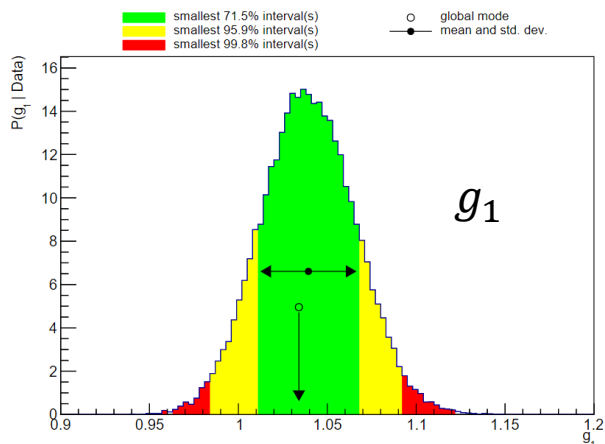
Then fix g_5 to new number, and fit for g_1, g_2, g_4, g_6 parameters again. After several iterations, choose the final parameters which is corresponding to the best χ^2 .



$$S_{IFY} = g_1 + (g_2 + g_3 b^2) \log\left(\frac{Q}{M_Z}\right) + g_4 \log\left(\frac{1960}{\sqrt{s}}\right) + g_5(\tanh(g_6 y_{Max}) + \tanh(g_6(|y| - y_{Max})))$$

Fitting results and Data/prediction comparison

fitting results on nonperturbative parameters



Parameter	Value
g_1	1.034 ± 0.026
g_2	0.053 ± 0.025
g_4	-0.143 ± 0.014
g_6	1.468 ± 0.108

Correlation matrix

$$C = \begin{pmatrix} 1 & 0.288 & -0.139 & 0.350 \\ 0.288 & 1 & 0.906 & -0.174 \\ -0.139 & 0.906 & 1 & -0.334 \\ 0.350 & -0.174 & -0.334 & 1 \end{pmatrix}$$

$$S_{IFY} = g_1 + (g_2 + g_3 b^2) \log\left(\frac{Q}{M_Z}\right) + g_4 \log\left(\frac{1960}{\sqrt{s}}\right) + g_5 (\tanh(g_6 y_{Max}) + \tanh(g_6 (|y| - y_{Max})))$$

$$g_3 = 0$$

$$g_5 = 13.45$$

Fitting results and Data/prediction comparison

➤ χ^2 results

Experiment	N_{pts}	χ^2 (IFY)	χ^2/dof (IFY)	χ^2 (SIYY)	χ^2/dof (SIYY)
CDF1	32	19.8	0.62	20.6	0.64
CDF2	41	48.5	1.18	62.6	1.53
D01	15	11.1	0.74	14.1	0.94
D02	8	19.4	2.43	21.9	2.74
E288 200	28	31.4	1.12	60.0	2.14
E288 300	35	34.6	0.99	42.0	1.20
E288 400	42	89.9	2.14	104.0	2.48
E605	35	54.5	1.56	71.1	2.03
R209	10	8.5	0.85	11.3	1.13
ATLAS	48	9.2	0.19	11.4	0.24
CMS	80	35.7	0.45	39.7	0.50
LHCb	10	18.3	1.83	23.2	2.32
Total	384	380.8	0.992	481.7	1.25

➤ SIYY refitting after including new data set

Parameter	Value
g_1	0.0 ± 0.004
g_2	0.773 ± 0.042
g_3	0.122 ± 0.006

Correlation matrix

$$C = \begin{pmatrix} 1 & 0.198 & -0.748 \\ 0.198 & 1 & -0.708 \\ -0.748 & -0.708 & 1 \end{pmatrix}$$

Previous results

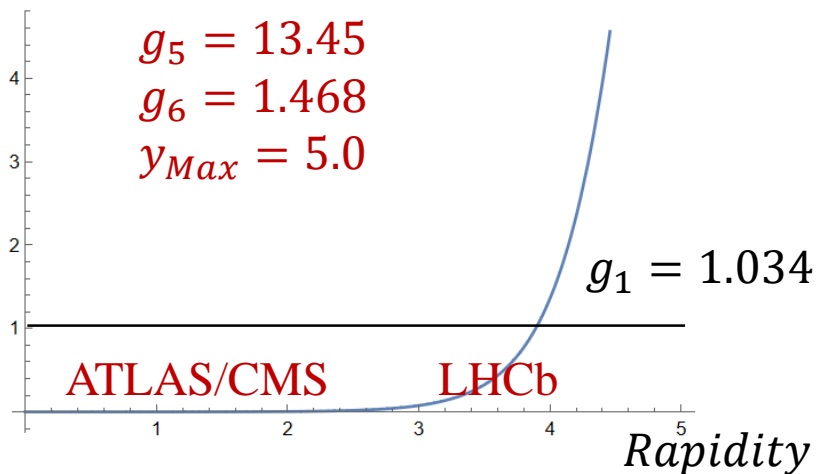
Parameter	SIYY fit
g_1	0.212
g_2	0.84
g_3	0.0

$$e^{-S_{NP}} = \exp \left[-g_1 b^2 - g_2 \ln(b/b_*) \ln(Q/Q_0) - g_3 b^2 \left((x_0/x_1)^\lambda + (x_0/x_2)^\lambda \right) \right],$$

[arxiv: 1406.3073](https://arxiv.org/abs/1406.3073)

Rapidity dependence in nonperturbative function

$$g_5(\tanh(g_6 y_{Max}) + \tanh(g_6(|y| - y_{Max})))$$

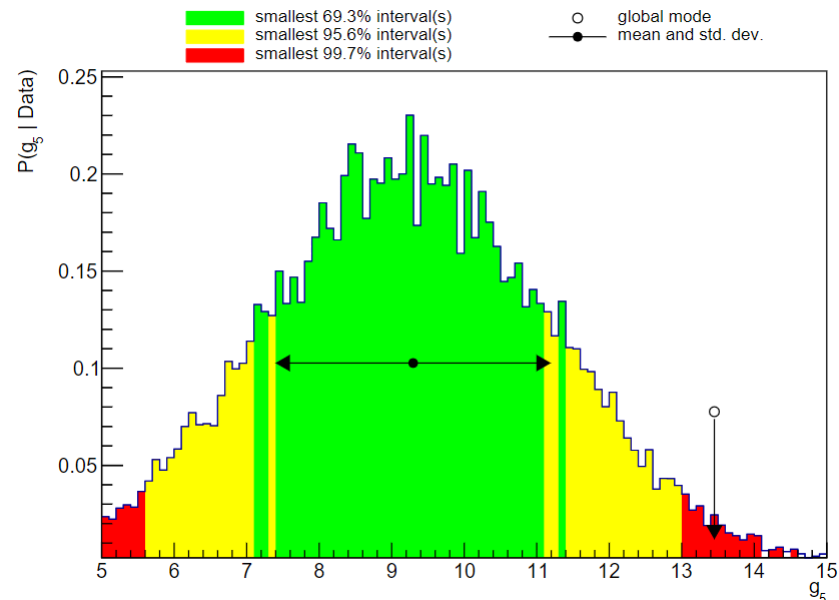


The g_5 (g_6) term is merely constrained by the LHCb data.

The χ^2 of each data point of LHCb data



χ^2	$g_5 = 0$	$g_5 = 13.45$
$p_T = 1.1$	1.422	0.042
$p_T = 2.8$	0.864	0.122
$p_T = 4.0$	2.666	2.086
$p_T = 5.2$	0.028	0.065

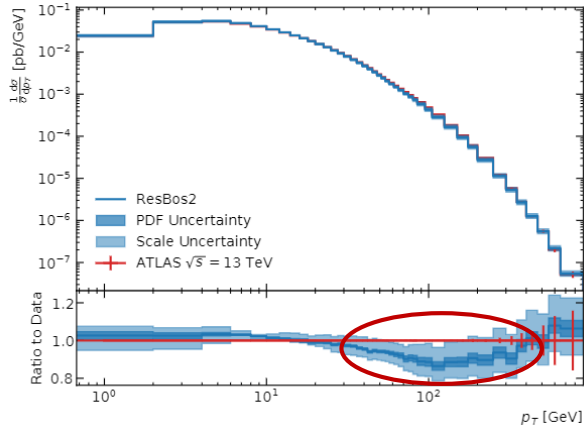


$$S_{IFY} = g_1 + (g_2 + g_3 b^2) \log\left(\frac{Q}{M_Z}\right) + g_4 \log\left(\frac{1960}{\sqrt{s}}\right) + g_5(\tanh(g_6 y_{Max}) + \tanh(g_6(|y| - y_{Max})))$$

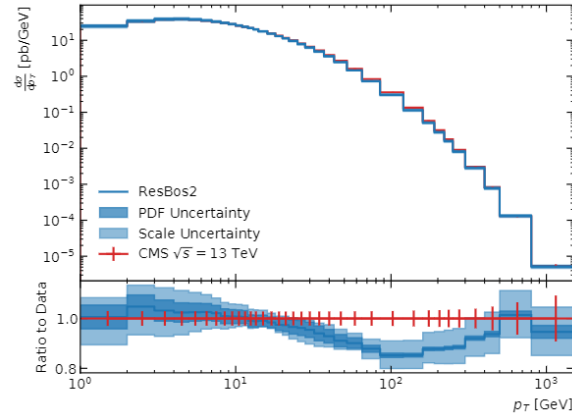
Fitting results and Data/prediction comparison

➤ Data/prediction comparison for LHC data

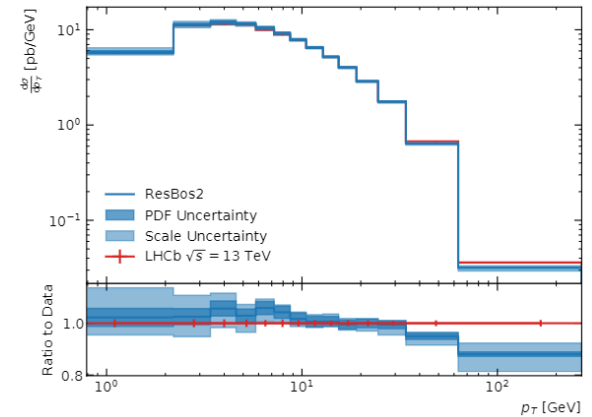
ATLAS



CMS



LHCb



The discrepancy in high p_T region is due to the missing of α_s^3 contribution.

We also did comparison for LHC 7/8/13 TeV data, all comparison look good. Detailed information is in the back-up.

Summary

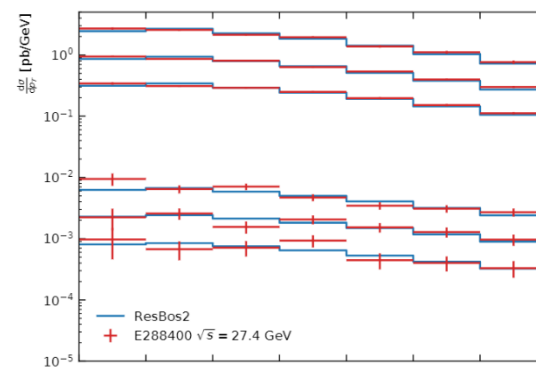
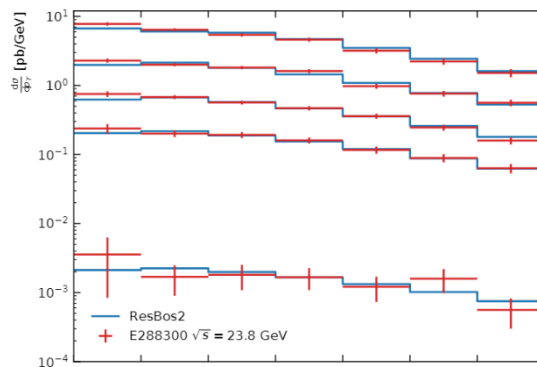
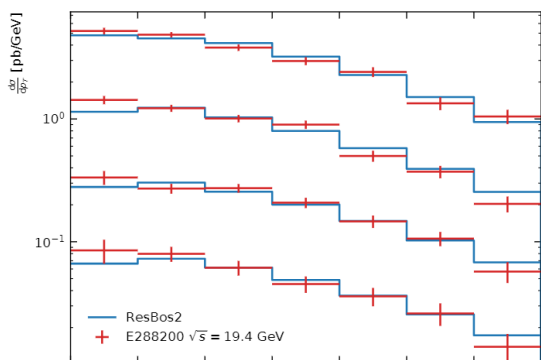
- The resummation order of ResBos2 has been updated to N3LL, a new nonperturbative fitting needs to be performed.
- A rapidity-dependent function is used in the nonperturbative fitting. New ATLAS, CMS, and LHCb rapidity-dependent data are included in the new fitting. Fitting results show the nonperturbative function has rapidity dependence.
- Data/prediction comparisons are shown using new ResBos2 calculation with new nonperturbative function. All the comparisons have good agreement.

Back up

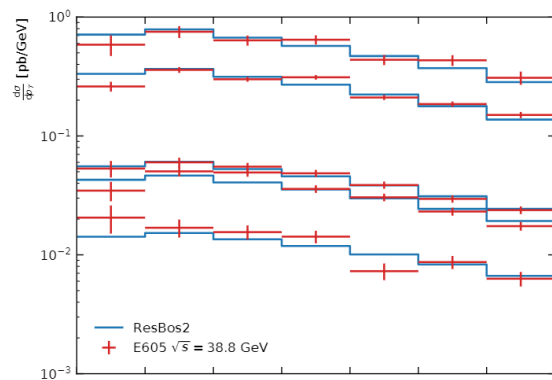
Fitting results and Data/prediction comparison

➤ Data/prediction comparison for low energy data

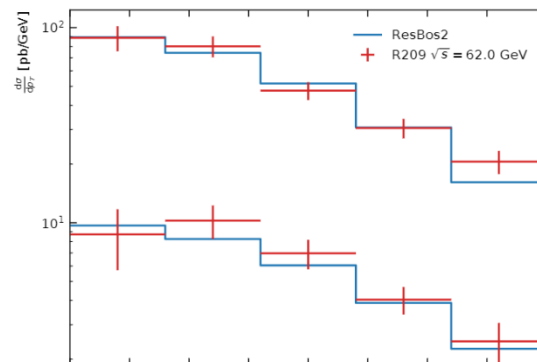
E288



E605



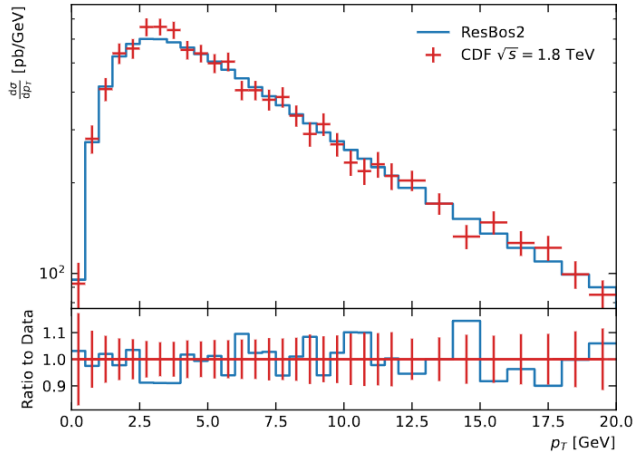
R209



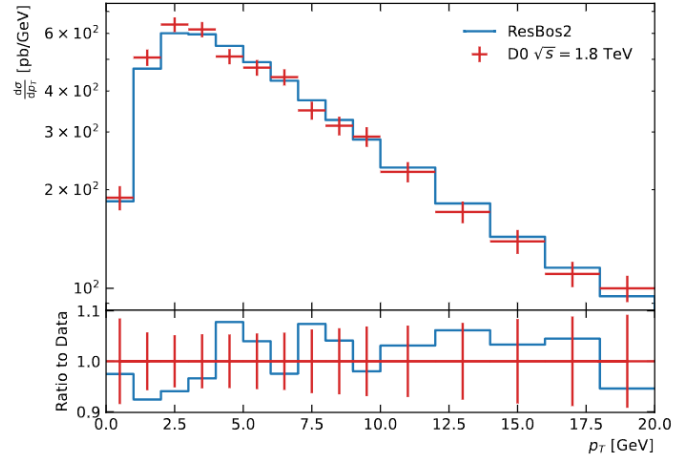
Fitting results and Data/prediction comparison

➤ Data/prediction comparison for Tevatron data

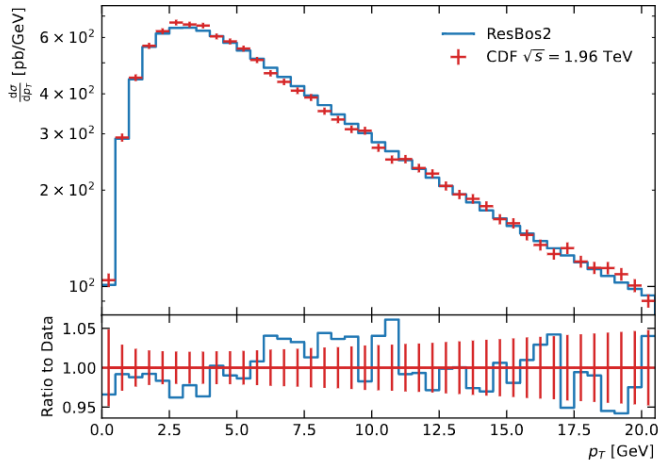
CDF I



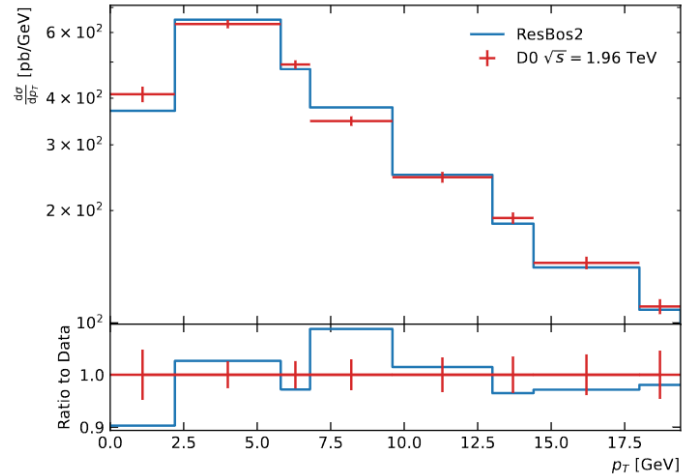
D0 I



CDF II



D0 II



Fitting results and Data/prediction comparison

➤ Data/prediction comparison for LHC data

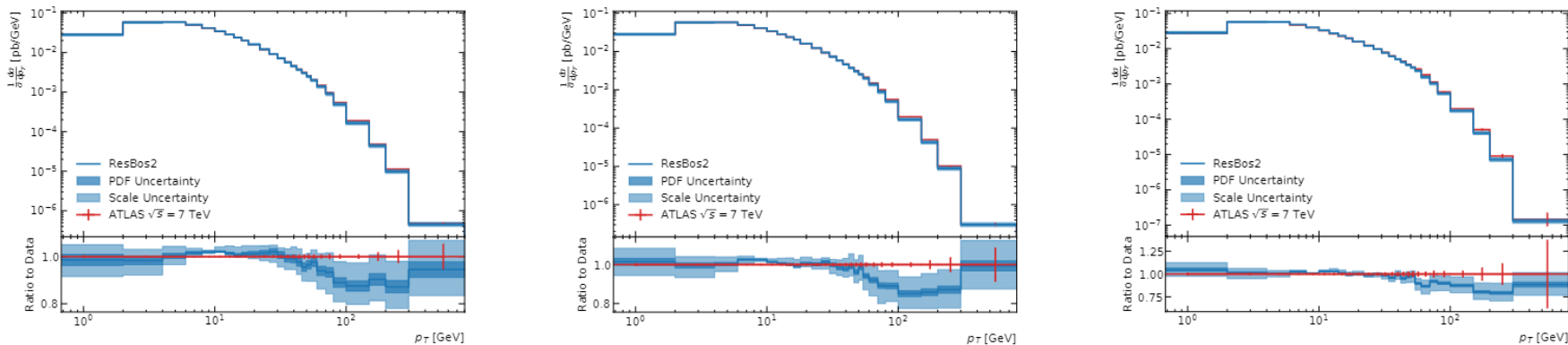


FIG. 9. Comparison between the ResBos2 calculation and the ATLAS 7 TeV p_T distributions from Ref. [82].

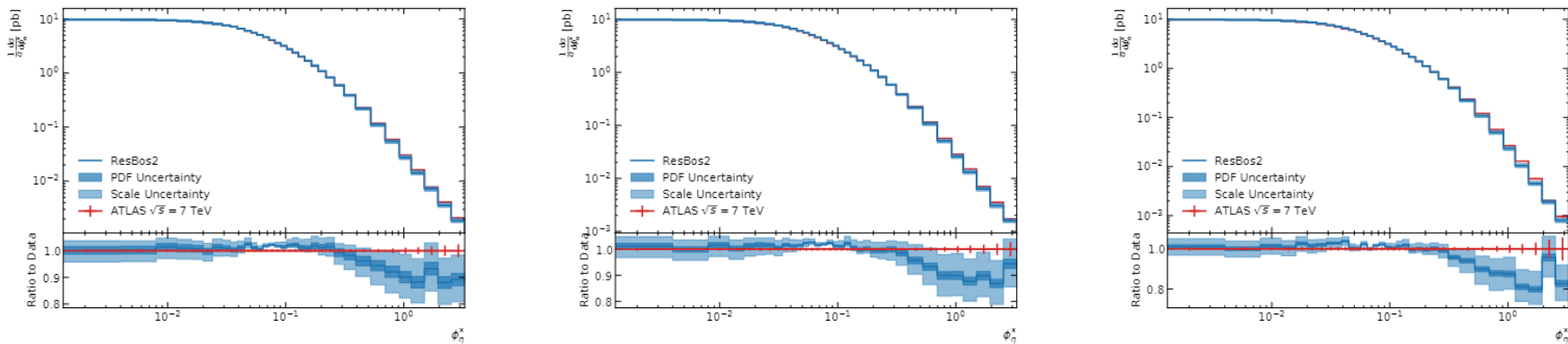


FIG. 10. Comparison between the ResBos2 calculation and the ATLAS 7 TeV ϕ_n^* distributions from Ref. [83].

Fitting results and Data/prediction comparison

➤ Data/prediction comparison for LHC data

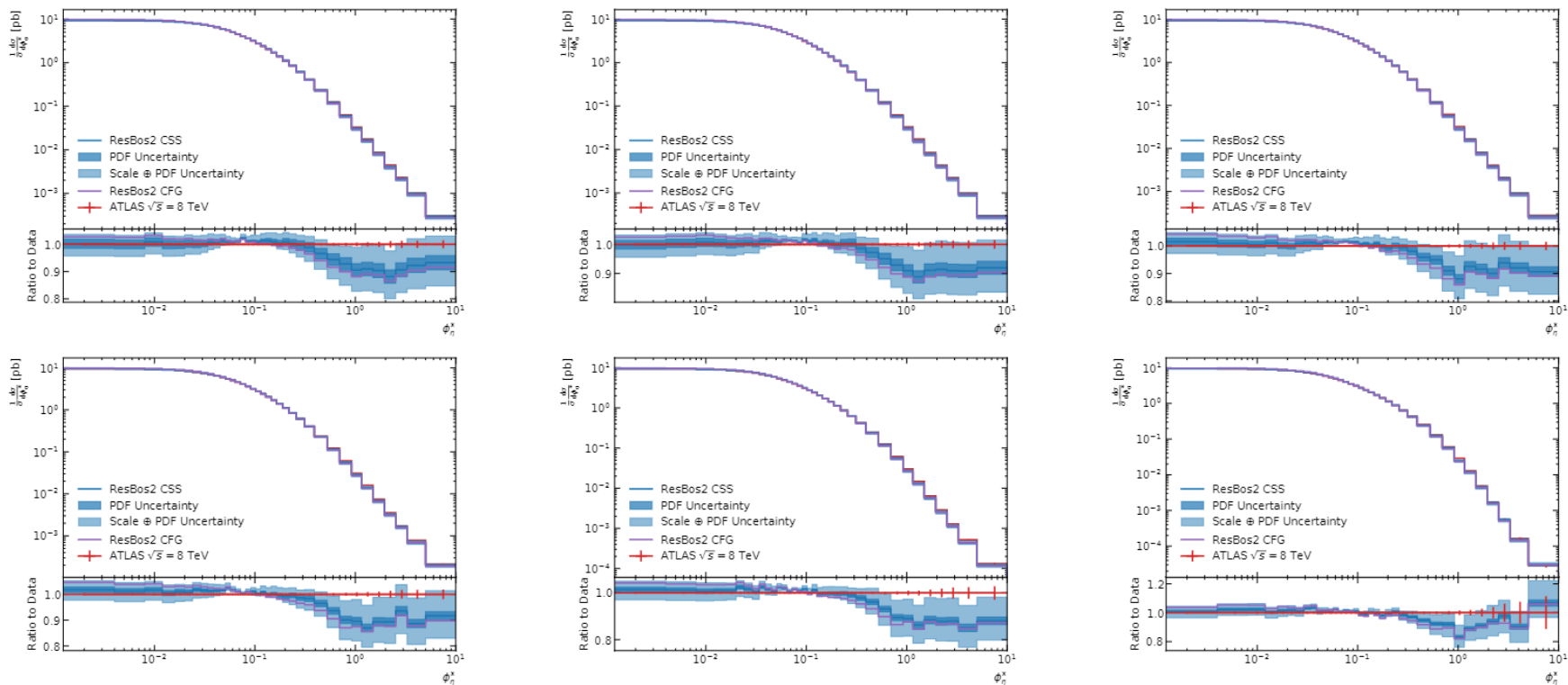


FIG. 12. Comparison between the ResBos2 calculation and the ATLAS 8 TeV ϕ_n^* distributions from Ref. [71].

Fitting results and Data/prediction comparison

➤ Data/prediction comparison for LHC data

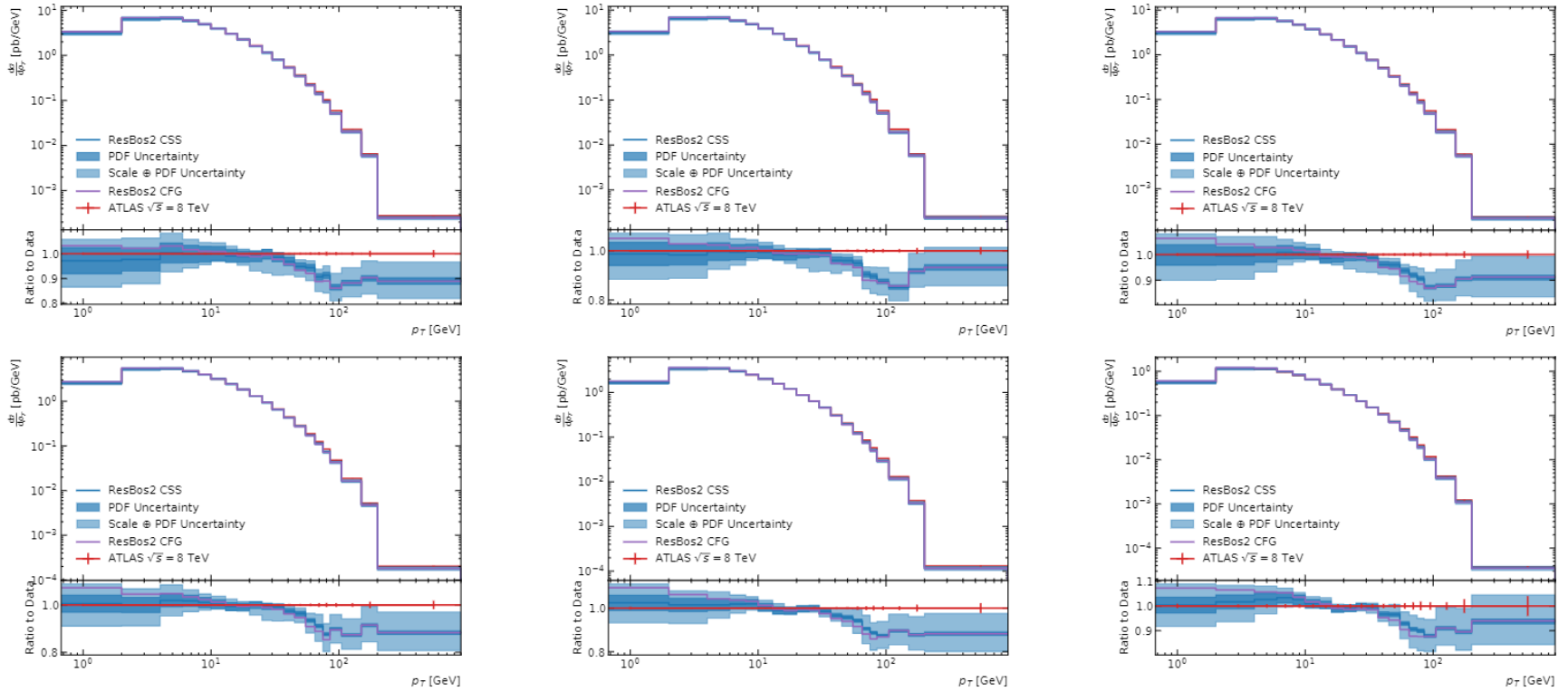


FIG. 13. Comparison between the ResBos2 calculation and the ATLAS 8 TeV p_T distributions from Ref. [71].

Fitting results and Data/prediction comparison

➤ Data/prediction comparison for LHC data

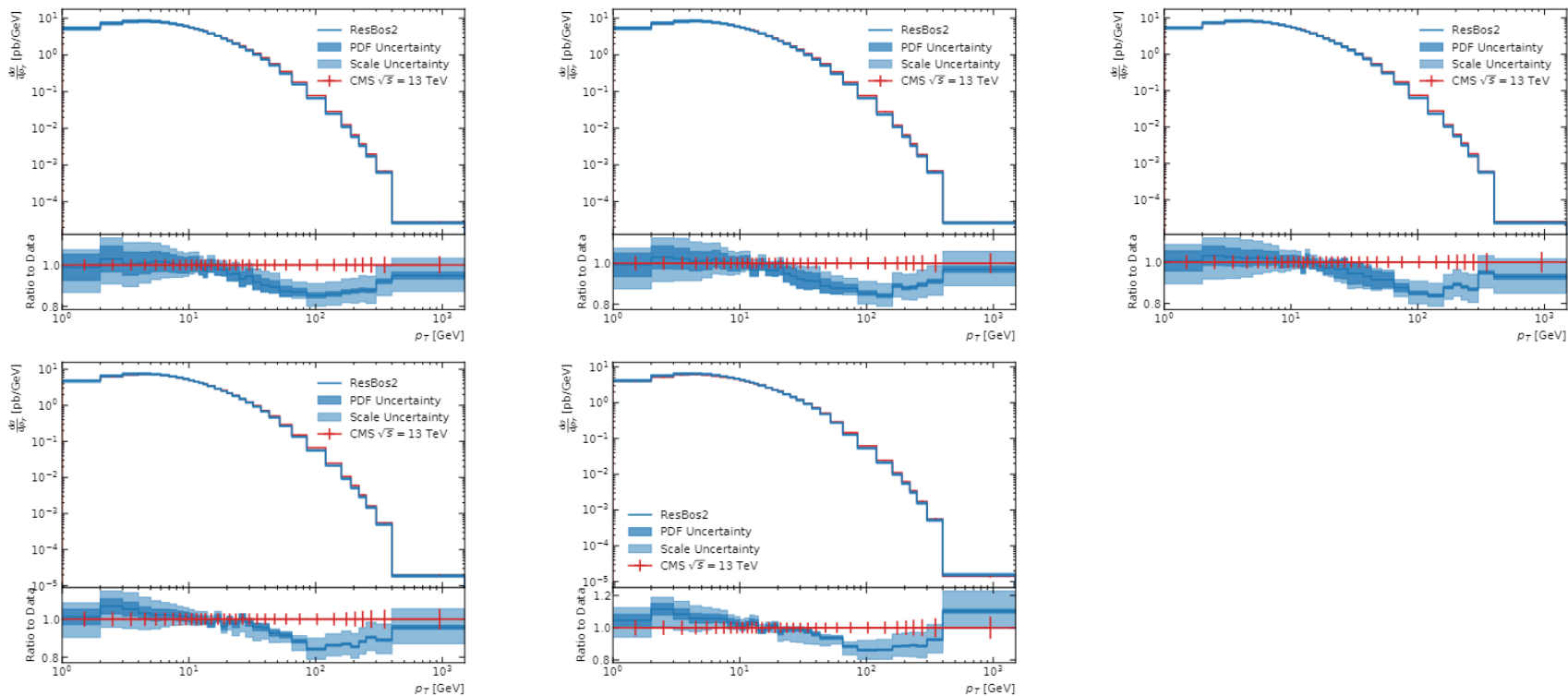


FIG. 15. Comparison between the Resbos2 calculation and CMS [2] for the p_T distribution in different rapidity bin.

Fitting results and Data/prediction comparison

➤ Data/prediction comparison for LHC data

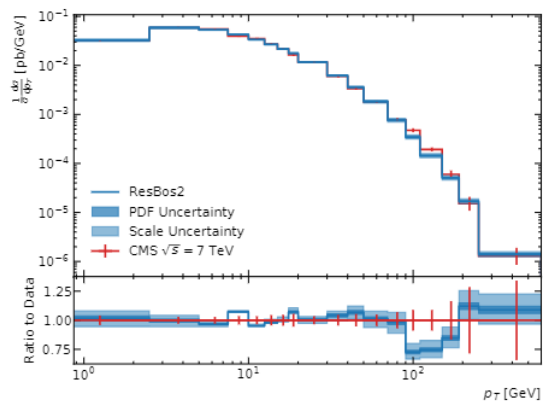


FIG. 11. Comparison between the ResBos2 calculation and the CMS 7 TeV p_T distributions from Ref. [84].

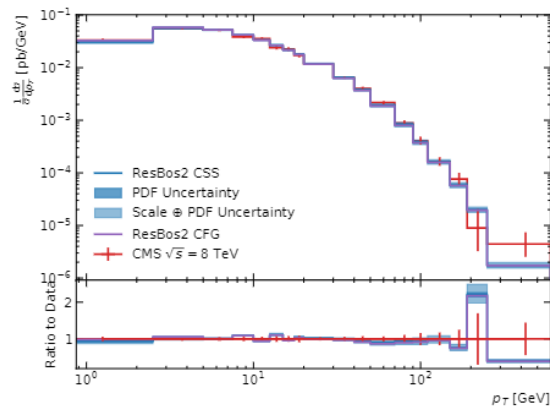


FIG. 14. Comparison between the ResBos2 calculation and the CMS 8 TeV p_T distributions from Ref. [86].